CGU HS Committee on River Ice Processes and the Environment
19th Workshop on the Hydraulics of Ice Covered Rivers
Whitehorse, Yukon, Canada, July 9-12, 2017.

River Ice Hydraulic Modeling of the Slave River Delta

Fan Zhang[1] and Karl-Erich Lindenschmidt[1]
[1]*Global Institute for Water Security, University of Saskatchewan*
11 Innovation Blvd, Saskatoon, Saskatchewan S7N 3H5
fan.zhang@usask.ca

Ice is an important component of hydraulic regimes of northern inland deltas such as the Slave River Delta. Ice jams and subsequent floodings can occur in the Slave River Delta during the breakup period, which is beneficial to the ecological integrity of the delta by replenishing the floodplain with moisture and sediment. To better understand the ice jam processes in the delta, RIVICE, a one-dimensional hydraulic river ice model, was implemented to simulate ice jam formation in the Slave River Delta. To determine essential inputs to RIVICE, such as incoming ice volume, downstream water level, bathymetry data, and upstream discharge, remote sensing technology and ground measurements were used. Gauge readings helped to calibrate and validate the RIVICE simulations. To evaluate the sensitivity of different parameters, a global sensitivity analysis (GSA) was carried on RIVICE parameters and boundary conditions. The sensitivity analysis reveals discharge to be the most sensitive factor on output variables such as backwater level profiles and the extent of ice jamming. The location of the ice jam toe, also, has a significant impact on ice jam processes, which has prompted more investigations on the impact of geomorphological factors on ice jam formation.

1. Introduction

River ice jamming and its consequential flooding is one of the key concerns for river hydraulic research in Canada and other cold regions. Ice jams can lead to higher water levels at relatively lower discharges than open water flooding, which poses higher risks to communities vulnerable to flooding (Lindenschmidt et al., 2016). Ice jam releases can lead to rapid advancement and accumulation of ice downstream to raise water levels more than would normally occur at the same flow for open water (Hicks, 2016; Nafziger et al., 2016). On the positive side, high water levels caused by ice jams can replenish perched basins in deltas with much needed moisture and sediment. After the construction of W.A.C Bennett Dam, a paucity of ice jam flooding reduced the replenishment and inundation effects in the Peace-Athabasca Delta in northern Alberta (Beltaos, 2014; Beltaos et al., 2006). The Slave River Delta, too, relies on the replenishment of moisture and sediment from ice jam flooding, just as the Peace-Athabasca Delta. Reduced flood frequency and drying periods in the Slave River Delta has been documented by previous research pointing to river regulation and climatic variations as possible causes (Brock et al., 2010). We pursued a direct field survey method, which has been proposed by Ambtman and Hicks (2012), to record ice jam profile and estimate hydraulic and physical properties that form them in this northern river.

In spite of the significance and value of ground-surveyed data in research, it is difficult and unsafe to do field measurements directly on ice jams. Hence, remote sensing technology helped support this research, technology often used to complement the dearth of direct measurement recordings. RADARSAT-2 images were used to measure river ice thicknesses along the Red River (Lindenschmidt et al., 2010), Saint-François River (Mermoz et al., 2014), and Mackenzie River (Mermoz et al., 2014). Chu et al. (2015) classified ice cover types of the Slave River Delta using RADARSAT-2 imagery. The optical sensor, MODIS, was used to monitor ice processes and breakup patterns along the Susquehanna River (Kraatz et al., 2016), Slave River (Chu & Lindenschmidt, 2016) and Mackenzie River (Mermoz et al., 2014).

To better understand the formation and development of ice jams in rivers, the river ice hydraulic model RIVICE was successfully applied to many cases such as the Lower Red River (Lindenschmidt et al., 2012) and the Peace River (Lindenschmidt et al., 2016), in which good agreement between simulation results and gauged data were obtained. To help support our modelling, HEC-RAS, a well-known hydraulic model developed by the Hydrologic Engineering Center, USACE, (Brunner, 2016), was also implemented. HEC-RAS has been operated for ice-jam-related flood events before, for example, in Beltaos et al. (2012). Comparison of HEC-RAS modelling results, such as discharge hydrographs, water levels, and runoff ice volumes with other model simulations and gauged data for model calibration have been carried out in previous studies (Hicks & Peacock, 2005).

Other studies have used sensitivity analysis to complement the modeling, for example, to evaluate the impact of geomorphology on river ice along the Dauphin River based on the RIVICE model (Lindenschmidt & Chun, 2013). Sensitivity analyses can also help quantify uncertainties in numerical modelling work. There are some different frameworks to setup sensitivity analyses, such as a Monte-Carlo framework (Saltelli et al., 2008), which was used in this study, and the VARS (Variogram Analysis of Response Surfaces) framework (Sheikholeslami et al., accepted).

RIVICE was set up to simulate ice jams in the Slave River Delta, in which parameter sensitivities were determined within a Monte-Carlo framework. RIVICE input and calibration data were acquired from Water Survey of Canada (WSC) and MODIS imagery. Once the model was calibrated and validated, a sensitivity analysis was carried out to determine the influence of parameters and boundary conditions on model output variables.

2. Study Site and Methods

2.1 Study Site

The Slave River flows from the confluence of the Peace River and Riviére des Rochers to Great Slave Lake. Approximately 66% of its annual flow stems from the Peace River (English et al., 1997). The Slave River, which drains the basins of the Peace River, Athabasca River, Lake Athabasca, and Peace-Athabasca Delta, provides 74% of the inflow to Great Slave Lake (Gibson et al., 2006). The whole Slave-Peace-Athabasca catchment drains approximately an area of 615,000 km^2. In general, the upper reach of the Slave River is relatively straight, while its lower reach is sinuous. This study focuses mainly on the river's mouth at the Slave River Delta (SRD), which is a wetland consisting of numerous river channels, braided islands and ponds. Five main channels extend throughout the Slave River Delta including the Resdelta, Middle, Steamboat and Nagle channels and the Jean River (Figure 1). The SRD is approximately 400 km^2 in area with the main channel flowing approximately 25 km in length through the delta. The SRD provides diverse habitats for various plants and animals. Local residential communities rely on the delta for their traditional lifestyle and livelihood by utilizing the natural resources of the delta (Elmes et al., 2016). Certain complex geomorphological features can be more prone to ice jamming in the SRD, which has been confirmed by other studies of the Slave River (Lindenschmidt & Das, 2015).

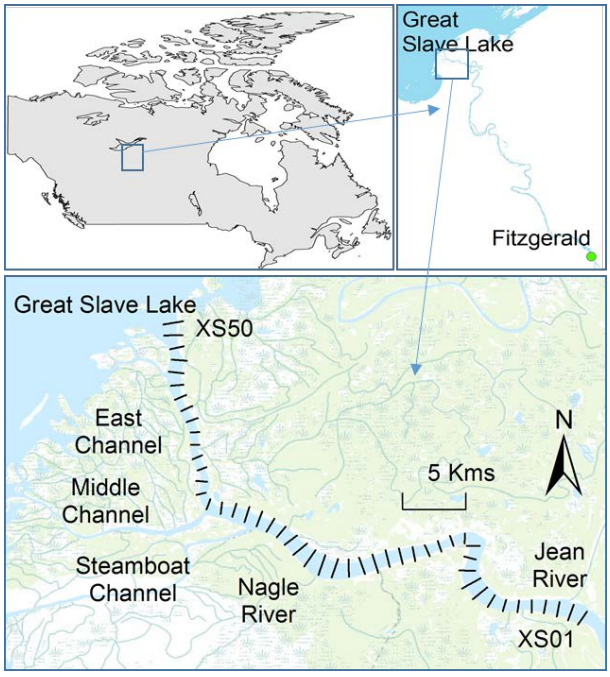

Figure 1. The Slave River Delta and cross-sections (XS) 1 to 50

The average river flow at Fitzgerald, which was used for the upper boundary condition flow in the simulations, has been modulated due to the construction of the W.A.C Bennett Dam. Figure 2 (left panel) shows the ice-on and ice-off dates for each winter between 1953 and 2010. The dates correspond to the first and last B-values accompanying the flow data for each winter. The B-values supplement the daily mean flow recordings when ice induces backwater effects on the flow at the gauge. The figure shows that there is no significant trend in the freeze-up and end-of-breakup dates with time. The mean freeze-up date is 6 November with a standard deviation of approximately ±10 days; the mean end-of-breakup date is 9 May with a standard deviation of ±7 days. Figure 2 (right panel) shows the day-average hydrographs extending over a year, from July to June, for both the pre-dam construction (1953-1970) and the post-dam construction (1973-2010) periods.

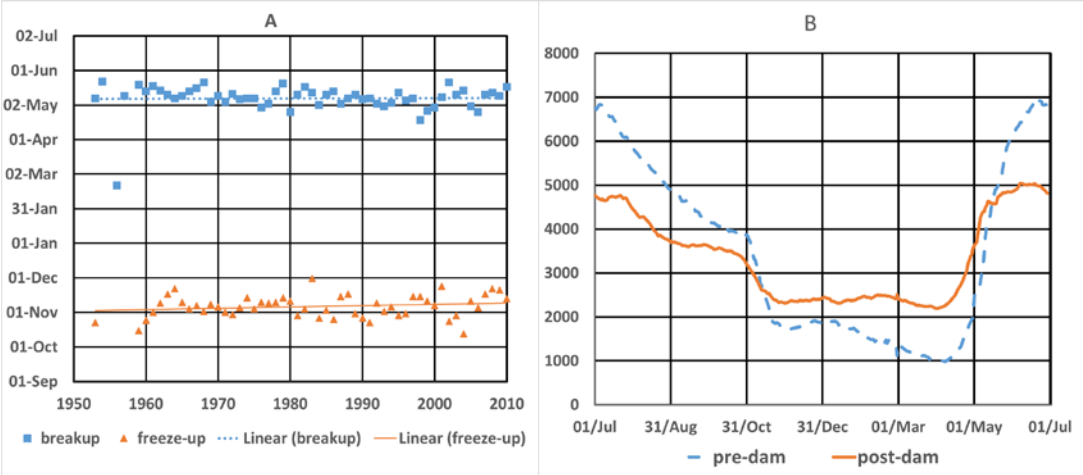

Figure 2. Left panel: Breakup and freeze-up dates between the years 1953 and 2010. Right panel: Mean flows for each day averaged over pre-dam (1953-1970) and post-dam (1973-2010) periods.

2.2 RIVICE model description

RIVICE is a one-dimensional hydrodynamic river ice model, which is used to simulate ice processes in rivers and channels, including frazil ice formation, juxtaposition of ice covers, shoving of ice at ice cover fronts, deposition and erosion of submerged ice, ice jams and hanging dams. Various equations, including Saint-Venant equations, Manning's equation, force balance equation, and other empirical equations are used in the RIVICE program to simulate transient flow conditions and ice cover development.

Two sources of ice for jamming are possible: frazil ice and inflowing ice from upstream of the jam. By calculating heat loss from the water surface, ice generation, ice transport, ice cover evolution, and other processes forming the ice cover profile can be simulated.

2.3 Data for Model Setup

Upper and lower bounds of parameters and boundary conditions used for the Global Sensitivity Analysis (GSA) are listed in Table 1. The range values were drawn from the RIVICE manual (KGS, 2013) and other publications (Lindenschmidt & Chun, 2013).

Table 1. Parameters and boundary conditions used in the RIVICE model (modified from Zhang et al., (2017)).

Parameters	Description	Units	Ranges
Hydraulic roughness			
n_{bed}	River bed roughness	s/m$^{1/3}$	0.025-0.035
n_{8m}	Ice roughness factor	s/m$^{1/3}$	0.09-0.13
Boundary conditions			
Q	Upstream discharge	m^3/s	2800-17000
W	Downstream water level	m a.s.l.	156.25-156.75
Ice cover characteristics			
v_d	Ice deposit velocity	m/s	1.1-1.3
v_e	Ice erosion velocity	m/s	1.7-1.9
v_{ice}	Inflowing ice volume	m^3	9-1000
FT	Thickness of ice cover front	m	0.15-0.35
PC	Porosity of ice cover	—	0.4-0.6
X	Ice bridge location (from XS1 in Figure 1)	m	100-480
h	Thickness of ice bridge	m	0.8-1.2
Strength properties			
K1TAN	Lateral: longitudinal stresses	—	0.11-0.22
K2	Longitudinal: vertical stresses	—	7-9
Slush ice characteristics			
PS	Porosity of slush	—	0.3-0.7
ST	Thickness of slush pans	m	0.3-0.8

2.4 Global Sensitivity Analysis (GSA)

Previous research used a local sensitivity analysis (LSA) to determine parameter and boundary condition sensitivities on output variables of ice jam simulations of the Slave River Delta (Zhang et al., 2017). In LSA, the model is first calibrated by manually changing parameters until simulated values reasonably match gauged data. When the model output is consistent with observed data, the parameter set of this model run is defined as the base run model. Then, each parameter or boundary condition value is changed one-at-a time using the same percentage for each model run. The percentage change of the output variable defines the parameter sensitivity. However, the LSA method is based on one specific base run parameter set and does not consider sensitivities within the entire parameter space. Thus, GSA was used to quantify the parameter sensitivity within the whole space. This was done using a Monte-Carlo approach.

The following equation was used to define the error ε between simulated and observed values: (Lindenschmidt & Chun, 2013):

$$\varepsilon = \sqrt{\frac{\Sigma(y_s - y_o)^2}{N}} \quad [1]$$

where y_s and y_o are simulated and observed values, respectively, N is the number of values, and ε is the error used as a criterion to distinguish between "*a priori* parameter set" and "behavioral parameter set". A primary parameter set without considering the error ε is defined as the *a priori* parameter set, while the selected parameter set based on ε value is defined as the behavioral parameter set. Cumulative distribution function plots (CDP) were used to show the distributions of the values used for each parameter set. The maximum

deviation between the *a priori* and the behavioral CDP defines the parameter sensitivity S. The magnitude of the parameter sensitivity equals the maximum distance between the two CDP curves shown conceptually in Figure 3. The left panel (A and D) shows an example of a non-sensitive parameter set where there is no difference between the *a priori* and behavioral parameter sets. Both the middle (B and E) and right (C and F) panels show sensitive parameter sets. However, when comparing the middle and right panels, the difference in the sensitive regions within the parameter spaces can be noticed. For some parameters, such as the ice bridge location in this research, the sensitive region is of importance. By comparing the lower panels of Figure *3* the sensitivity within the entire range of parameter values can be seen, not just at one parameter setting such as in the local sensitivity analysis.

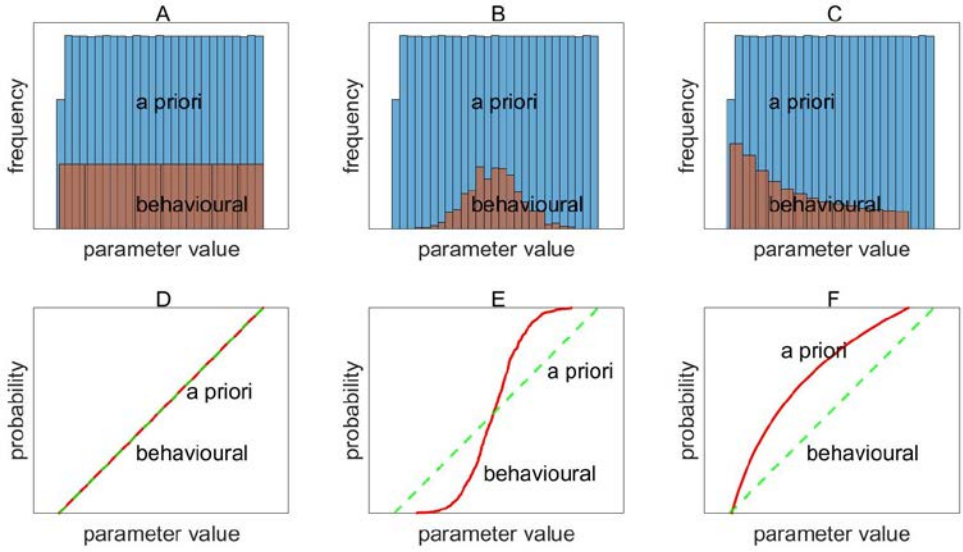

Figure 3. Cumulative distribution plots of behavioral and *a priori* parameter sets

Among all 15 parameters and boundary conditions, an important one is the upstream discharge of the river. According to the Extreme value theory (Gumbel, 2004) as well as flood stage frequency curve analysis (Lindenschmidt et al., 2015), a Gumbel distribution can be fit to the discharge data, in particular to our short data series. However, uniform distributions are often solely used for GSA methods, such as VARS, which requires all input distributions of the parameters and boundary conditions to be uniform. Therefore, in our SRD modeling case, both Gumbel and uniform distributions of discharge were used to setup the Monte Carlo simulations for comparison, called the Gumbel Scenario and Uniform Scenario hereafter. This distinction is necessary for a subsequent study comparing Monte-Carlo (regional) global sensitivity analysis with VARS (Zhang and Lindenschmidt, in prep).

3. Results and Discussion

For the SRD river ice modeling, 15 parameters listed in Table 2 were chosen to carry out nearly 1000 Monte Carlo simulations. Output variables from succeeded runs (837 results for Gumbel Scenario and 694 results for Uniform Scenario) were extracted for the subsequent analysis. Variables include water level profiles and ice jam cover extents.

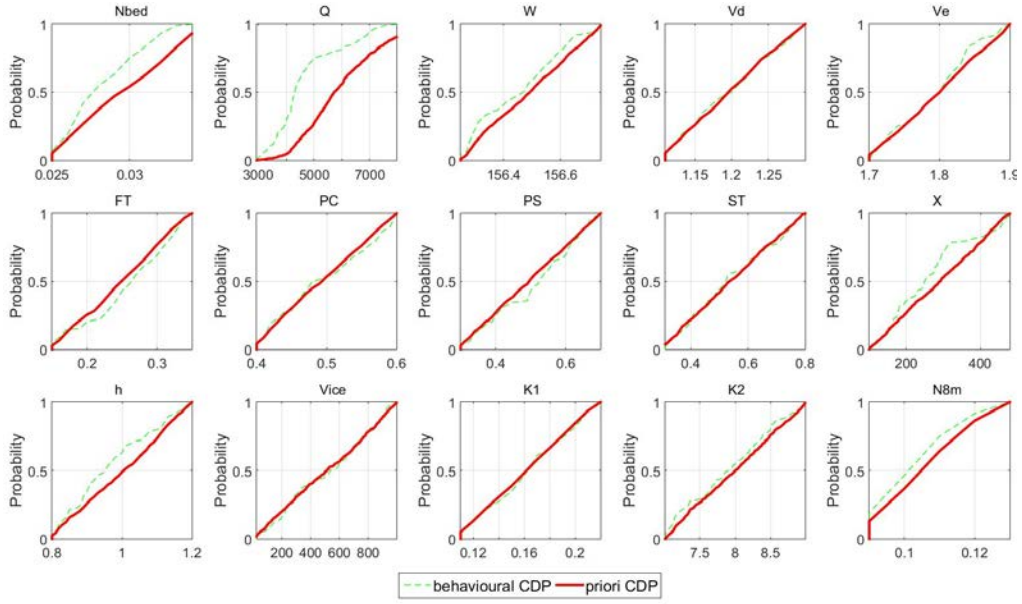

Figure 4. Cumulative distribution plots (CDP) under Gumbel Scenario

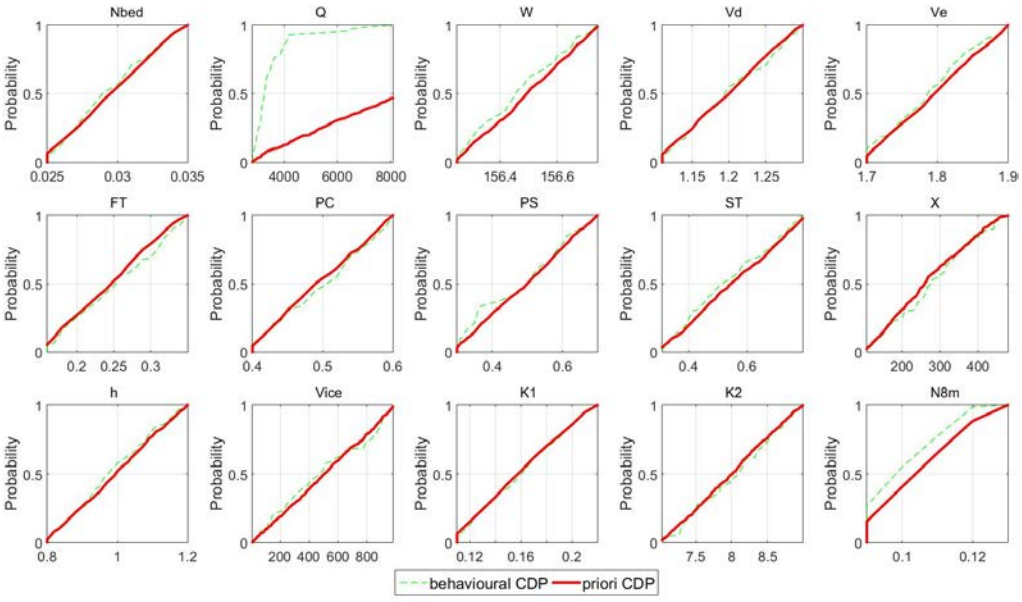

Figure 5. Cumulative distribution plots (CDP) under Uniform Scenario

Table 2. Global sensitivities and rankings

	Gumbel Scenario		Uniform Scenario	
Parameters	Sensitivity	Rank	Sensitivity	Rank
Nbed	0.070	8	0.034	11
Q	0.491	1	0.442	1
W	0.099	5	0.074	5
Vd	0.003	14	0.019	14
Ve	0.061	10	0.075	4
FT	0.098	6	0.077	3
PC	0.020	12	0.056	8
PS	0.070	8	0.067	6
ST	0.002	15	0.029	12
X	0.129	3	0.058	7
h	0.164	2	0.048	10
Vice	0.022	11	0.020	13
K1	0.019	13	0.017	15
K2	0.078	7	0.053	9
N8m	0.119	4	0.169	2

As Figures 4 and 5 show, discharge Q is very sensitive in both the Gumbel and Uniform Scenarios. Ice roughness factor n_{8m}, riverbed roughness n_{bed}, ice bridge location x, and ice bridge thickness h are sensitive in the Gumbel Scenario. In the Uniform Scenario, the most sensitive parameters are ice roughness factor n_{8m} and discharge Q. The difference may be due to the greater weighting given to extreme high discharges in the uniform distribution. When discharge is distributed uniformly, the extreme high discharges occur as frequently as low discharges. The sensitivity of ice bridge location x indicates the distinct effect of geomorphological conditions on ice jamming. The downstream boundary condition, water level W is not quite as sensitive since the water level of Great Slave Lake changes mildly. By comparing the average of *a priori* parameter sets with behavioral ones, the difference in boundary condition Q is noticeable. This difference further confirms the sensitivity of Q, since extreme high discharges led to ice cover front shoving. High discharges also led to higher backwater levels.

It is clear that the flow has been moderated with the construction of the dam, with summer flows being capped and winter flows having increased (Figure 2, left panel). However, during the time of average ice-on and ice-off dates, the two curves intersect; hence, there is no definitive distinction in the flows during the freeze-up and end-of-ice period. Beltaos (2014) states that both dropping the freeze-up water level and increasing the discharge at breakup can lead to increased severity of ice jamming and subsequent flooding. In fact, the flows prior to the breakup and delta are on average, higher after dam construction than the natural flow condition. Hence, this may be a case for the severity and frequency of ice jamming along the Slave River having increased or at least remaining the same. However, the increase in the flow rate during the breakup period before the dam construction was much faster, which, we argue can also make ice breakup and jamming more severe. Hence, it is difficult to determine how the severity of ice jam flooding may have been affected by the flow regulation of the upper Peace River.

4. Conclusion

The boundary condition, upstream discharge Q, is the most sensitive parameter determined from the GSA. The distribution of discharge affects not only sensitivity of the discharge itself but also other parameter and boundary condition sensitivities, such as x (ice bridge location). According to previous research (Lindenschmidt & Chun, 2013), the location of the ice bridge is related to the geomorphological setting of the river, however, the effects of river flow on the ice bridge location was not found. The physical explanation of the relationship of the upstream discharge distribution and the ice bridge location still requires further research.

The sensitivity of boundary condition Q indicates the possibility of maintaining or even increasing the ice jamming frequency and severity by water regulation. We suggest that maintaining high discharge at breakup may help retain ice jam severity in the delta.

References

Ambtman, K. D., & Hicks, F., 2012. Field estimates of discharge associated with ice jam formation and release events. Canadian Water Resources Journal, 37(1): 47-56.

Beltaos, S., 2014. Comparing the impacts of regulation and climate on ice-jam flooding of the Peace-Athabasca Delta. Cold Regions Science and Technology, 108: 49-58.

Beltaos, S., Prowse, T. D., & Carter, T., 2006. Ice regime of the lower Peace River and ice-jam flooding of the Peace-Athabasca Delta. Hydrological Processes, 20(19): 4009-4029.

Beltaos, S., Tang, P., & Rowsell, R., 2012. Ice jam modelling and field data collection for flood forecasting in the Saint John River, Canada. Hydrological Processes, 26(17): 2535-2545.

Brock, B. E., Martin, M. E., Mongeon, C. L., Sokal, M. A., Wesche, S. D., Armitage, D., Edwards, T. W. D., 2010. Flood frequency variability during the past 80 years in the Slave River Delta, NWT, as determined from multi-proxy paleolimnological analysis. Canadian Water Resources Journal, 35(3): 281-300.

Brunner, G. W., 2016. HEC-RAS river analysis system-hydraulic reference manual, US Army Corps of Engineers, Hydrologic Engineering Center

Chu, T., Das, A., & Lindenschmidt, K. E., 2015. Monitoring the variation in ice-cover characteristics of the Slave River, Canada using RADARSAT-2 data-A case study. Remote Sensing, 7(10): 13664-13691.

Chu, T., & Lindenschmidt, K. E., 2016. Integration of space-borne and air-borne data in monitoring river ice processes in the Slave River, Canada. Remote Sensing of Environment, 181: 65-81.

Elmes, M. C., Wiklund, J. A., Van Opstal, S. R., Wolfe, B. B., & Hall, R. I., 2016. Characterizing baseline concentrations, proportions, and processes controlling deposition of river-transported bitumen-associated polycyclic aromatic compounds at a floodplain lake (Slave River Delta, Northwest Territories, Canada). Environmental Monitoring and Assessment, 188(5): 282.

EC., 2013. RIVICE model-User's manual. (http://giws.usask.ca/rivice/Manual/RIVICE_Manual_2013-01-11.pdf)

English, M. C., Hill, R. B., Stone, M. A., & Ormson, R., 1997. Geomorphological and botanical change on the Outer Slave River Delta, NWT, before and after impoundment of the Peace River. Hydrological Processes, 11(13): 1707-1724.

Gibson, J. J., Prowse, T. D., & Peters, D. L., 2006. Hydroclimatic controls on water balance and water level variability in Great Slave Lake. Hydrological Processes, 20(19): 4155-4172.

Gumbel, E. J., 2004. Statistics of extremes (Dover edition. ed.). Mineola, N.Y.: Dover Publications.

Hicks, F. E., 2016. An Introduction to River Ice Engineering: For Civil Engineers and Geoscientists: CreateSpace Independent Publishing Platform.

Hicks, F. E., & Peacock, T., 2005. Suitability of HEC-RAS for Flood Forecasting. Canadian Water Resources Journal / Revue canadienne des ressources hydriques, 30(2): 159-174.

Kraatz, S., Khanbilvardi, R., & Romanov, P., 2016. River ice monitoring with MODIS: Application over Lower Susquehanna River. Cold Regions Science and Technology, 131: 116-128.

Lindenschmidt, K. E., & Das, A., 2015. A geospatial model to determine patterns of ice cover breakup along the Slave River1. Canadian Journal of Civil Engineering, 42(9): 675-685.

Lindenschmidt, K. E., Syrenne, G., & Harrison, R., 2010. Measuring Ice Thicknesses along the Red River in Canada Using RADARSAT-2 Satellite Imagery. Journal of Water Resource and Protection, 02(11): 923-933.

Lindenschmidt, K. E., & Chun, K. P., 2013. Evaluating the impact of fluvial geomorphology on river ice cover formation based on a global sensitivity analysis of a river ice model. Canadian Journal of Civil Engineering, 40(7): 623-632.

Lindenschmidt, K. E., Das, A., Rokaya, P., & Chu, T. A., 2016. Ice-jam flood risk assessment and mapping. Hydrological Processes, 30(21): 3754-3769.

Lindenschmidt, K. E., Sydor, M., Carson, R. W., & Harrison, R., 2012. Ice jam modelling of the Lower Red River. Journal of Water Resource and Protection, 04: 11.

Lindenschmidt, K. E., Apurba, D; Rokaya, P; Kwok, C; Chu, T., 2015. Ice jam flood hazard assessment and mapping of the Peace River at the Town of Peace River. 18th Workshop on the Hydraulics of Ice Covered Rivers organized by CRIPE - Committee on River Ice Processes and the Environment, Quebec City, QC, Canada, August 18-20, 2015.

MacLean, A. J., Tolson, B. A., Seglenieks, F. R., & Soulis, E., 2010. Multiobjective calibration of the MESH hydrological model on the Reynolds Creek Experimental Watershed. Hydrology and Earth System Sciences Discussions, 7(2): 2121-2155.

Mermoz, S., Allain-Bailhache, S., Bernier, M., Pottier, E., Van Der Sanden, J. J., & Chokmani, K., 2014. Retrieval of River Ice Thickness From C-Band PolSAR Data. IEEE Transactions on Geoscience and Remote Sensing, 52(6): 3052-3062.

Nafziger, J., She, Y. T., & Hicks, F., 2016. Celerities of waves and ice runs from ice jam releases. Cold Regions Science and Technology, 123: 71-80.

Pietroniro, A., Fortin, V., Kouwen, N., Neal, C., Turcotte, R., Davison, B., Pellerin, P., 2007. Development of the MESH modelling system for hydrological ensemble forecasting of the Laurentian Great Lakes at the regional scale. Hydrology and Earth System Sciences, 11(4): 1279-1294.

Prowse, T. D., Conly, F. M., Church, M., & English, M. C., 2002. A review of hydroecological results of the Northern River Basins Study, Canada. Part 1. Peace and Slave rivers. River Research and Applications, 18(5): 429-446.

Saltelli, A., Ratto, M., Andres, T., Campolongo, F., Cariboni, J., Gatelli, D., Tarantola, S., 2008. Global Sensitivity Analysis: The Primer. John Wiley & Sons, Ltd.

Sheikholeslami, R., Yassin, F., Lindenschmidt, K. E., Razavi, S., accepted. Improved Understanding of River Ice Processes Using Global Sensitivity Analysis Approaches. Journal of Hydrologic Engineering.

Zhang, F., Mosaffa, M., Chu, T., Lindenschmidt, K. E., 2017. Using Remote Sensing Data to Parameterize Ice Jam Modeling for a Northern Inland Delta. Water, 9(5): 306.
Zhang, F. Lindenschmidt, K-E., In prep. Comparison of Regional Sensitivity Analysis and VARS for Global Sensitivity Analysis of a River ice model of an Inland Delta.